



# Research on the sustainable measurement of machined surface roughness under the influence of cutting environment

Wei Chen<sup>1,2,3,4</sup> · Bin Zou<sup>1,2,3,4</sup> · Qinbing Zheng<sup>1,2,3,4</sup> · Chuanzhen Huang<sup>5</sup> · Lei Li<sup>1,2,3,4</sup> · Jikai Liu<sup>1,2,3,4</sup>

Received: 14 February 2023 / Accepted: 10 June 2023 / Published online: 29 June 2023  
© The Author(s), under exclusive licence to Springer-Verlag London Ltd., part of Springer Nature 2023

## Abstract

The machined surface in the industrial cutting environment is often covered by some interference factors, such as chips or coolant residuals, which make the existing methods have large detection errors. Therefore, the interference factors in the cutting environment seriously affect the sustainability detection and evaluation of the processed surface quality. This paper discusses the relationship between interference factors and roughness to study the sustainability detection of roughness. Firstly, a multidimensional feature parameter matrix with strong correlation with surface roughness is extracted and constructed based on the gray level co-occurrence matrix. On this basis, the adverse effects of interference factors (chips) on image feature parameters are quantitatively analyzed. According to the relationship between chip area and error change rate of feature parameters, an error correction model is constructed to optimize the feature parameters that change due to interference factors. The error correction model greatly reduces the negative influence of chip interference. This is the core of this paper. Further, the BP neural network model and support vector machine (SVM) model are used to predict the surface roughness with the optimized multi-dimensional feature parameters matrix as input, respectively. The above process realizes the sustainable detection of machined surface roughness. At the same time, in order to facilitate industrial applications, this paper uses LabVIEW software and MATLAB software to package the above research into a software system. Finally, the practicability and effectiveness of the sustainable detection research are verified by practical application in the industrial scene. This study promotes the sustainable development between product safety and environmental impact in the industrial manufacturing process.

**Keywords** Interference factors · Sustainability roughness detection · Error correction model · Feature parameter optimization

## 1 Introduction

With the development of industrial automation and intelligence [1, 2], the research on sustainability detection of machined surface quality is getting more and more attention in the industrial manufacturing process. It is closely related to the safety of the workpiece during use. Surface roughness, as one of the evaluation indicators of the quality of the machined surface, affects the future performance and service life of the product [3, 4], and it is also an indispensable part of sustainable detection research. In addition, the sustainable detection of surface roughness during the industrial manufacturing process can also take remedial measures in advance for the damage caused by the out-of-control machining process [5]. This can increase the safety and economy of the product after manufacture.

✉ Bin Zou  
zb78@sdu.edu.cn

- <sup>1</sup> Centre for Advanced Jet Engineering Technologies (CaJET), School of Mechanical Engineering, Shandong University, 17923 Jingshi Road, Jinan 250061, China
- <sup>2</sup> Key Laboratory of High Efficiency and Clean Mechanical Manufacture, Shandong University, Ministry of Education, 17923 Jingshi Road, Jinan 250061, China
- <sup>3</sup> National Demonstration Center for Experimental Mechanical Engineering Education, Shandong University, 17923 Jingshi Road, Jinan 250061, China
- <sup>4</sup> Additive Manufacturing Research Center of Shandong University of National Engineering Research Center of Rapid Manufacturing, Shandong University, 17923 Jingshi Road, Jinan 250061, China
- <sup>5</sup> Yanshan University, Qinhuangdao 066000, China

Although existing detection methods have good accuracy, their better accuracy depends on the ideal laboratory environment. In the actual industrial environment, interference factors, such as chips, on the industrial site will cover the defects, bringing great adverse effects on the sustainability detection of surface roughness [6]. Therefore, the sustainability detection of surface roughness under the influence of interference factors is considered one of the major challenges in the field of detection. The main contribution of this paper is to make it possible to sustainability detection of machined surface roughness under the influence of interference factors. The research process is more robust than existing research.

In this paper, the influence of interference factors that often occur in the cutting environment on the feature parameters is quantitatively analyzed. The error correction model was constructed by studying the relationship between chip area and error rate of feature parameters. The error correction model can optimize the feature parameters changed by the influence of interference factors. The error correction model greatly reduces the negative impact of chip interference. This is the core of this paper. Further, the BP neural network model and support vector machine (SVM) model are used to predict surface roughness with the optimized multi-dimensional feature parameters matrix as input, respectively. The above process realizes the sustainable detection of machined surface roughness.

This paper is organized as follows. In Section 2, some advanced research contents of surface roughness measurement are briefly reviewed. In Section 3, the surface image acquisition process under the influence of the industrial cutting environment is described. In Section 4, a multi-dimensional feature parameter matrix with strong correlation with roughness is constructed. In Section 5, the influence degree of interference factors on feature parameters is quantitatively analyzed, and the error correction model is innovatively proposed. In Section 6, two surface roughness prediction models are constructed. In Section 7, the research on the sustainability detection of surface roughness is systematically integrated. Finally, the conclusions are provided in Section 8.

## 2 Related works

The existing research on surface roughness detection focuses on non-contact detection. Such methods may include ultrasonic method, capacitance measurement method, and optical technology method (laser triangulation method, speckle method, scattering method, and machine vision). Balasundaram and Ratnam [7] proposed an online measurement system for turning surface roughness. The system is equipped with a SLR camera to collect surface images.

He uses a SLR camera to take a picture of the surface and extracts the contour of the cutting surface through the gray matrix edge threshold algorithm to obtain the contour curve. Then, the roughness is calculated according to the roughness parameter calculation formula. Tootooni et al. [8] proposes an on-line detection method of surface roughness based on machine vision. During the study, images of different regions of the rotation axis are obtained online using the camera. Then, changes in surface roughness are tracked online using algebraic graph theory image processing. The error of the proposed method in the actual detection process can be guaranteed within 15%. Liu et al. [9] developed a DSP-based surface roughness online detection system, which solved the problem of slow speed and low accuracy in online surface roughness detection of grinding workpieces. The system collects surface scattering images by industrial camera and pre-processing and feature parameter extraction using DSP chip. Finally, the surface roughness is predicted using the support vector machine model. Yi and Zhang [10] proposes a detection method for surface roughness based on machine vision techniques and image processing techniques. Computing pixel intensity of online collected images using MATLAB software. Then, the correlation between pixel intensity and surface roughness is explored. In addition, other scholars have done some research on data fusion [11, 12].

With the increasing complexity of industrial automation application scenarios, the actual application effect of the above research is decreasing. How to maintain the sustainable detection of surface roughness in complex environments is an important research direction. Some scholars have studied robust surface roughness detection. Deng et al. [13] studied the detection of surface quality of concrete bridges affected by interference. In this study, an ad hoc YOLO v2 network is proposed to detect concrete cracks and handwriting interference on the surface of concrete bridges. The handwriting interference is added to the collected defect image. Then, the network is trained to detect real flaws in complex contexts and interference. The results of this study show that the YOLO v2 could automatically locate cracks and measure roughness with bounding boxes from raw images, even with handwritten scripts. At the same time, the network's mAP is 77%. Although YOLO v2 has proved to be robust in concrete surface quality detection with relatively fast speed, the algorithm still needs further improvement to achieve real-time evaluation of concrete surface quality, and the detection accuracy is poor. Pashmforoush and Bagherinia [14] studied the effect of environmentally friendly water-based copper nanofluids on the grinding performance of Inconel 738 superalloy. To evaluate the effectiveness of this nanofluid, the wheel load ratio and surface roughness values were compared with dry grinding and conventional fluid grinding using image processing techniques. The results

showed that the application of copper nanofluids could improve wheel loading and surface roughness by amount of 59.19% and 62.16% compared to dry grinding and by amount of 35.13% and 36.36% respectively compared to conventional fluid grinding.

Liu et al. [15] solved the problem that environmental vibration has a great impact on traditional phase-shifting interferometry (PSI) for roughness measurement. Based on the iterative algorithm that is tolerant to phase-shifting error caused by vibration, the authors developed two interferometers to measure the optical surface figure and roughness respectively. The actual test shows that the error of roughness ( $S_q$ ) measured in the vibration, 0.4 micron-amplitude, and over 0–20Hz frequency range is less than 0.5 nm. The developed method and instruments could be applied to optical surface measurement in vibration. However, the robustness of this method is not good. An anti-interference roughness detection method based on image repair and convolutional neural network model was proposed by Yang et al. [16]. This method combines the CNN model, CBAM Res Net semantic segmentation model, and PConv Net image painting model. The experimental results show that the surface roughness detection accuracy of this method is 90.0% under the influence of interference factors. This method depends on the regular texture structure, with poor detection accuracy.

In addition, some scholars have also explored and found the feature parameters with strong correlation with roughness and anti-interference. Yi et al. [17] proposed a method to predict surface roughness by using average color difference feature parameters based on the overlapping structure of red and green colors through mechanism analysis of color image features. The robustness of this color feature parameter in disturbed and polluted environments is investigated. Although polluted, the authors found that the correlation between this feature parameter and surface roughness is much higher than those of other traditional feature parameters. The regression model based on the support vector machine is used to verify the effectiveness of the proposed method. However, this method needs to build a more complex red and green environment and is affected by monochromatic interference, which is not suitable for industrial promotion and application. Yi et al. [18] explored the influence of color information on metal surface roughness. The authors constructed the color distribution statistical matrix based on the multi-dimensional and red-green color aliasing structure of color image information. Based on the color distribution statistical matrix, the aliasing area index and the pure color area energy index which have a great relationship with roughness are extracted. Then, the performance of the two indexes in accuracy, stability, and anti-interference is comprehensively evaluated.

On the one hand, robust surface defect detection investigations require further research on detection accuracy and stability. On the other hand, the key to research is to consider the factors that negatively affect sustainability detection. The results obtained from the study separated from the actual interference factors cannot help to maintain the sustainability of surface roughness detection research. In this paper, it is found that chip interference often occurs in industrial cutting environments. Therefore, the contribution of this paper is to consider the actual interference factors in the industrial field. The error correction is made to feature parameters that are changed due to interference factors. The error correction fundamentally solves the adverse effect of interference factors on surface roughness measurement.

### 3 Acquisition and preprocessing of the sample image dataset

The basis of the measurement research is a lot of cutting surface images. This section obtained a sufficient number of sample blocks through milling experiments. The material used in the milling experiments is superalloy (GH4169). This process selects the clean cutting mode of high-speed dry milling. Machine tool is the CNC machining center of DMG company in Germany. It is found that the cutting process of per tooth feed and cutting speed are the most important influences on the surface roughness. Referring to the tool manual, 60 m/min and 90 m/min are selected as cutting speed, and 5 groups of parameters are selected as feed per tooth between 0.05 and 0.25 mm/z.

When the milling work is finished, the different regions of the finished surface image are obtained by laser microscope as the sample surfaces. The magnification of the laser microscope is 200 times. At the same time, the roughness of the sample surfaces was measured by VK microscope analysis software. Finally, each sample surface has a corresponding roughness value. This forms the original sample surface dataset. The surface roughness of the dataset is distributed in the range of 0.5  $\mu\text{m}$  and 2.0  $\mu\text{m}$ . The surface image size is 1980  $\times$  960 pixels. The visual view of the actual image is 1.413 mm  $\times$  1.060 mm. The dataset is divided into two parts: the non-interference sample surface image dataset and sample surface image dataset group. Among them, a non-interference surface image and its corresponding surface image having chip interference are a group. The chips on the surface are randomly assumed. Some of the larger chips produced during the milling process will leave the machined surface with the tool rotating. The experimental scheme process is shown in Fig. 1. The experimental site and the process of obtaining surface data are shown in Fig. 2.

**Fig. 1** Experimental scheme process

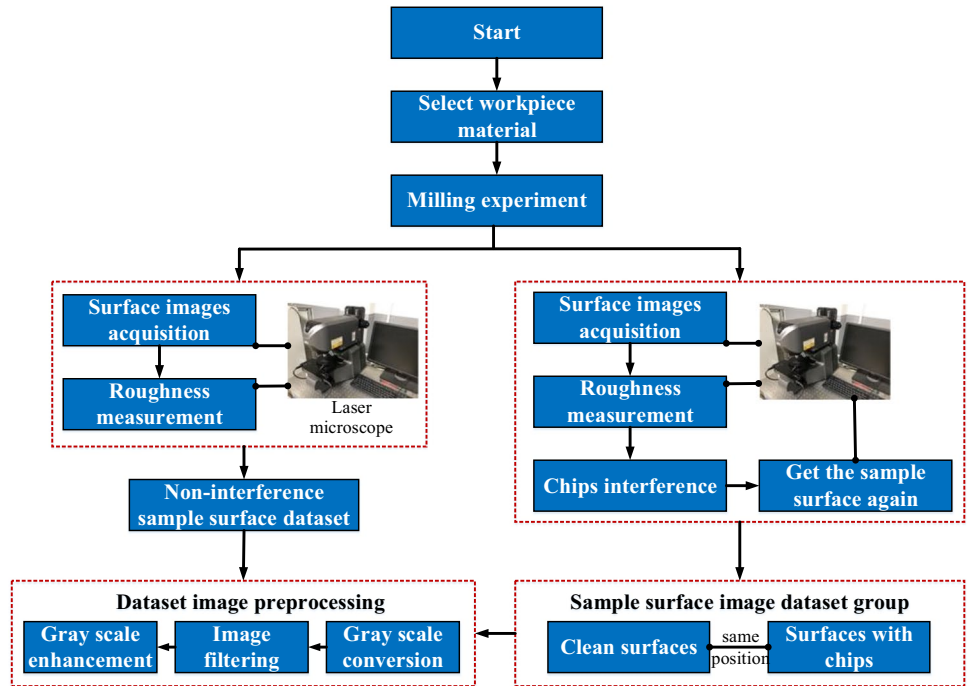
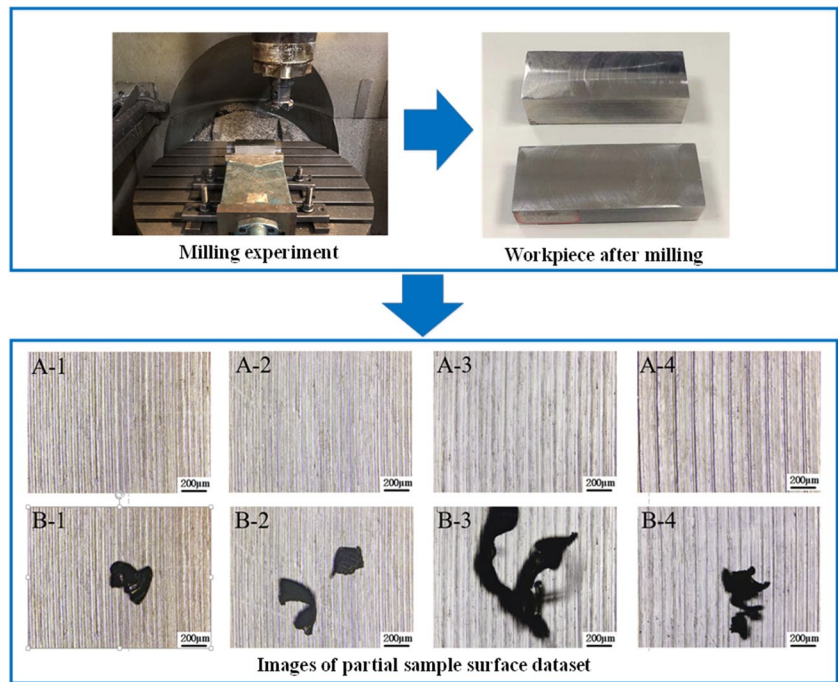


**Fig. 2** Work site and the acquisition process of the surface images



Because the image acquisition and transmission process is easily affected by light, machine tool vibration and other factors, the collected original image can not be directly used for analysis. Therefore, the collected surface image must be preprocessed to eliminate interference

information. The image preprocessing includes three parts: gray scale conversion, image filtering, and gray scale enhancement. The image preprocessing process is implemented based on LabVIEW software. The image preprocessing process is shown in Fig. 3.

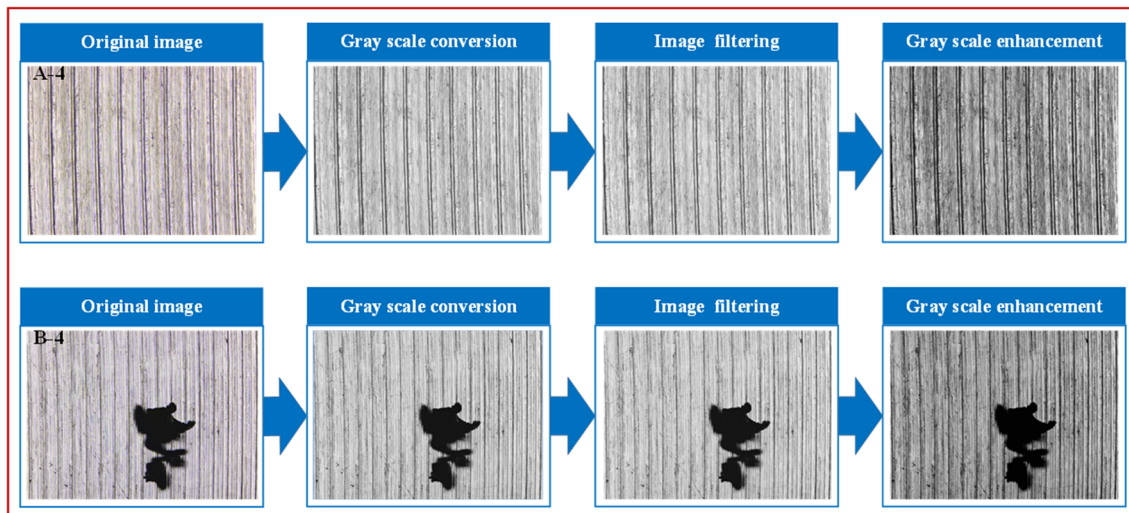


Fig. 3 Image preprocessing process

## 4 Construction process of multi-dimensional feature parameters matrix

### 4.1 Feature parameters extraction of surface images based on the gray level co-occurrence matrix

The prediction of surface roughness depends on the effective surface characteristics. The basic features of the surface include texture features, shape features, and color features. Textured features are widely used because they are a more complete reflection of surface information. Extraction of texture features usually uses the gray level co-occurrence matrix. Gray level co-occurrence matrix is a typical statistical method used to describe the distribution law of image gray scale values. The gray level co-occurrence matrix was proposed by Haralic et al. [19].

Based on the research of existing scholars, the surface texture is characterized by the six statistics commonly used in the gray level co-occurrence matrix. The six statistics are energy, contrast, entropy, homogeneity, differences, and correlations. During the study, six feature parameters of the gray level co-occurrence matrix in the  $0^\circ$  direction are extracted for each image. The grayscale is 32 and the growth step is 1. The above process is implemented by LabVIEW software.

### 4.2 Construction of a multi-dimensional feature parameters matrix

Six feature parameters of 110 non-interference sample surfaces in the dataset are extracted by the gray level co-occurrence matrix. To investigate whether there is a good

correlation between feature parameters and roughness, the six feature parameters and surface roughness are curve fitted by the least square method. The criterion for fitting is to meet the monotonicity between surface roughness and feature parameters.

The fitting results ( $R^2$ ) of six feature parameters, difference, contrast, entropy, homogeneity, correlations, and energy with roughness, are 0.8089, 0.8613, 0.8557, 0.2771, 0.06171, and 0.8990 respectively. The closer  $R^2$  is to 1, the better the fitting result of the model. It can be seen that the fitting results of difference, contrast, entropy, and energy exhibit better. Therefore, the multi-dimensional feature parameters matrix  $X$  should be constructed from the above four parameters to characterize the surface texture feature information.

$$X = [\lambda_{dif}, \lambda_{con}, \lambda_{ent}, \lambda_{ene}]^T \quad (1)$$

where  $\lambda_{dif}$  is the difference feature parameter,  $\lambda_{con}$  is the contrast feature parameter,  $\lambda_{ent}$  is the entropy feature parameter, and  $\lambda_{ene}$  is the energy feature parameter.

### 4.3 Quantitative analysis of the influence of interference factors (chips) on feature parameters

When detecting in the machine tool cutting phase of the industrial manufacturing process, the surface will be covered by some interference factors, such as chips and coolant residuals. These will have adverse effects in the process of extracting multi-dimensional feature parameters matrix. This section provides a quantitative analysis of the adverse effects of interference factors on feature parameters. Figure 4 is a set of preprocessed images selected from the dataset.

**Fig. 4** Images of different chip sizes

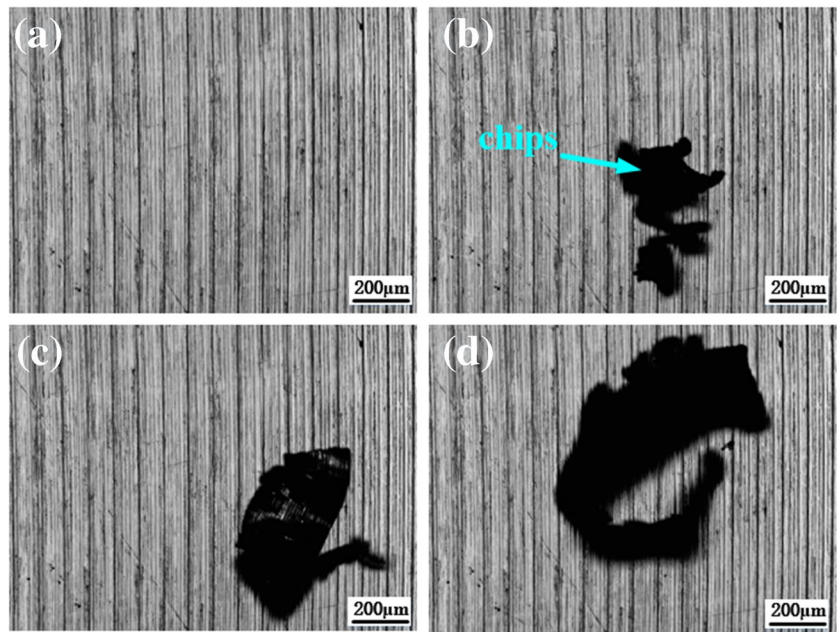


**Table 1** Feature parameters of images with different chips sizes

Number	Difference	Contrast	Entropy	Energy ( $10^{-3}$ )
a	2.0434	11.2814	5.3450	9.5417
b	1.8870 (−7.65%)	10.2641 (−9.02%)	5.2583 (−1.62%)	11.9414 (+25.15%)
c	1.7536 (−14.18%)	9.6425 (−14.53%)	5.0472 (−5.57%)	32.5471 (+241.1%)
d	1.6278 (−20.34%)	9.0206 (−20.04%)	4.8457 (−9.34%)	45.4154 (+376.0%)

Among them, Fig. 4a is an image without chip interference, and Fig. 4b–d are a set of images after adding chip interference of different sizes. Table 1 shows the multi-dimensional feature parameters of this set of images extracted using a gray level co-occurrence matrix. It can be seen from the relative error in the table that the feature parameters of the image have changed to varying degrees when disturbed by chips. Therefore, if the surface roughness cannot be detected for sustainability under interference factors, it will have a great safety hazard for the performance of the products after manufacturing.

## 5 Optimization process of feature parameters based on the error correction model

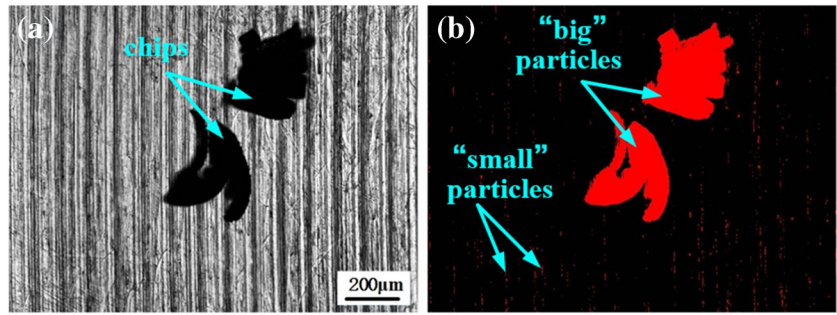
### 5.1 The construction process of the error correction model

Through the results in Section 4.3, the chip causes errors in the extracted feature parameters. Therefore, this section will construct an error correction model to eliminate

the adverse effects of interference factors. Specifically, the quantitative calculation of the image chip area is taken as the entry point. Then, the functional relationship between the error change rate of each feature parameter and the chip area can be obtained. Furthermore, the error correction model of feature parameters is established based on the functional relationship.

The chip area calculation process is as follows. Firstly, the images were binarized. After binarization, the image includes three parts: the “large” particle part, the “small” particle, and the background part. The above three parts are all composed of individual pixels. The “particles” are areas with gray values belonging to a class and connected with each other in the binarized image. The chip region can be regarded as “big” particles, and the influence region of other original texture structures can be regarded as “small” particles. The particles are shown in Fig. 5. Then, the chip area can be represented by calculating the area sum of all “large” particles in the binarized image. The area of “large” particles is the total number of pixels contained within them. Among them, the pixel number of “large” particles is counted by the four-connected region method. The distinction line between “large” particles and “small” particles is 1000 pixels, meaning that greater than

**Fig. 5** Binarization of surface image



1000 pixels are “large” particles, and otherwise “small” particles.

The error change rate of the feature parameters  $\alpha$  is calculated according to the Equation (2).

$$\alpha = \frac{|\lambda_{chip} - \lambda|}{\lambda} \tag{2}$$

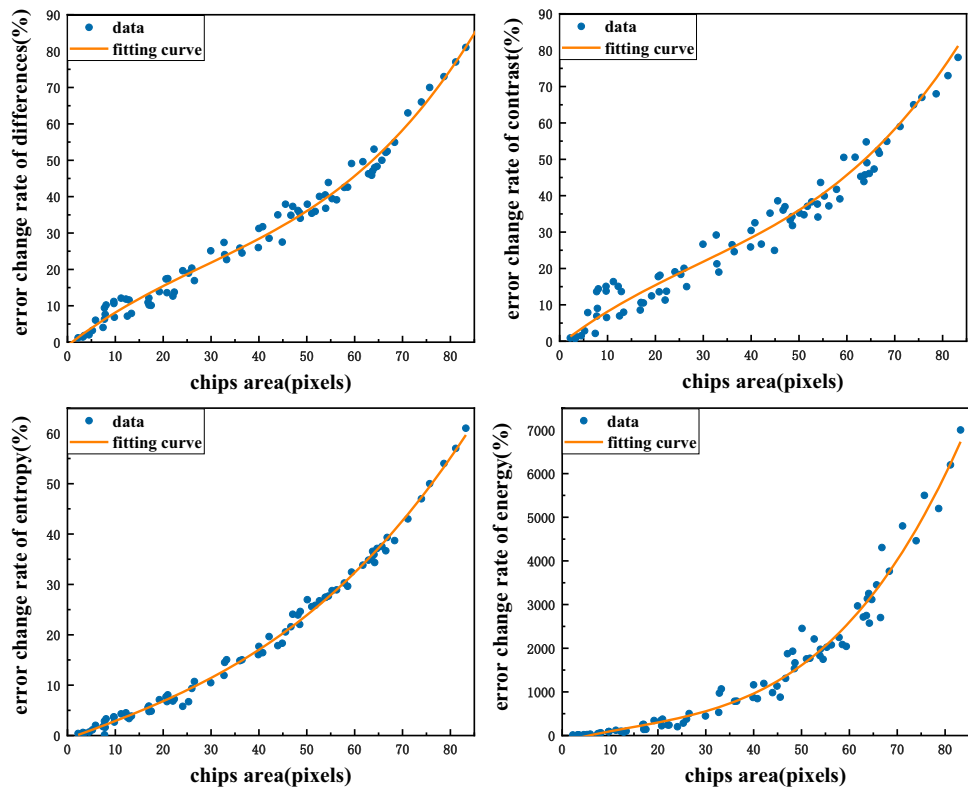
where  $\lambda$  is the feature parameter of the non-interference image and  $\lambda_{chip}$  is the feature parameter of its corresponding image with chip interference.

Figure 6 shows the relationship between the chip area and the error change rate of each feature parameter, which is obtained from 80 images with chips interference. According to Fig. 6, it is known that the error change rate of the feature parameters is controlled within 10% when the chip

area of the image is less than 50,000 pixels. Therefore, this case does not require an error correction to the feature parameters. The error change rate of feature parameters is more than 10% when the chip area of the image is between 50,000 and 700,000 pixels. This shows that the error in the feature parameters must be corrected. The error change rate of feature parameters is extremely large when the chip area of the image is greater than 700,000 pixels. This shows that it is necessary to reselect a new surface for roughness measurement.

The least squares method is used to fit the error change rate of the four feature parameters of 70 images with chip interference (the chip area is between 50,000 and 700,000 pixels) and the chips area. Fitting results ( $R^2$ ) of the error change rate of feature parameters difference, contrast, entropy, and energy with roughness are 0.9769, 0.9423,

**Fig. 6** Relation curve between the chip area and the error change rate of the feature parameters



0.9927, and 0.9508, respectively. According to the fitting results, the functional relationship between the error rate of change of each feature parameter and the chip area can be obtained. The functional relationships are shown in Equation (3).

$$\begin{cases} \alpha_{dif} = f_{dif}(S) = 2.874 \times 10^{-3}S^2 + 0.5386S + 2.775 \\ \alpha_{con} = f_{con}(S) = 4.53 \times 10^{-3}S^2 + 0.3808S + 5.45 \\ \alpha_{ent} = f_{ent}(S) = 5.376 \times 10^{-3}S^2 + 0.2111S + 0.2305 \\ \alpha_{ene} = f_{ene}(S) = 0.9603S^2 - 17.19S + 165.9 \end{cases} \quad (3)$$

The above relations are all monotonic functions, and the independent variable and the dependent variable have a unique corresponding relationship. Therefore, the error correction model of the feature parameters is expressed in Equations (4) and (5).

$$\begin{cases} \lambda_{optimized-dif,con,ent,ene} = \frac{\lambda_{chip-dif,con,ent,ene}}{1 \pm \alpha_{dif,con,ent,ene}} \\ \alpha_{dif,con,ent,ene} = f_{dif,con,ent,ene}(S) \\ S = \sum N_{0pixel} \end{cases} \quad (4)$$

$$\begin{cases} \lambda_{optimized-dif} = \frac{\lambda_{chip-dif}}{1 - \alpha_{dif}}, \lambda_{optimized-con} = \frac{\lambda_{chip-con}}{1 - \alpha_{con}}, \lambda_{optimized-ent} = \frac{\lambda_{chip-ent}}{1 - \alpha_{ent}}, \lambda_{optimized-ene} = \frac{\lambda_{chip-ene}}{1 + \alpha_{ene}} \end{cases} \quad (5)$$

the pre-optimized feature parameters, the average error of contrast is 4.04%, difference average error is 5.18%, entropy average error is 2.51%, and energy average error is 8.86%. These results show that the error correction model has a good effect on the optimization of feature parameters and proves the effectiveness of the error correction model. According to the results, the proposed error correction model can effectively optimize the changed feature parameters. The error correction model realizes the necessary premise for the sustainable detection of surface roughness.

## 6 Surface roughness prediction based on machine learning methods

According to the above research, the feature parameters changed due to interference factors being optimized by the error correction model, which makes it possible to successfully use machine learning methods to predict surface roughness. The prediction models based on machine learning methods mainly include BP neural network model, SVM model, and deep convolution neural network model.

On the one hand, although the deep convolution neural network model can automatically extract features, it needs a

where  $S$  is the chip area and  $N_{0pixel}$  is the sum of particle areas above 10,000 pixels after image binarization processing.  $\lambda_{chip-dif}$ ,  $\lambda_{chip-con}$ ,  $\lambda_{chip-ent}$ ,  $\lambda_{chip-ene}$  are the four feature parameters of the image with chip interference, respectively.  $\lambda_{optimized-dif}$ ,  $\lambda_{optimized-con}$ ,  $\lambda_{optimized-ent}$ ,  $\lambda_{optimized-ene}$  are the optimized four feature parameters, respectively. Then, because the difference, contrast, and entropy decrease with chip area, the denominator of  $\lambda_{optimized-dif}$ ,  $\lambda_{optimized-con}$ ,  $\lambda_{optimized-ent}$  in Equation (5) is negative. Because the energy increases with chip area, the denominator of  $\lambda_{optimized-ene}$  in Equation (5) is positive.

In conclusion, the error correction of image with chip interference (chip area between 50,000 and 700,000 pixels) requires the following process: (1) calculate the chip area of the image; (2) the error correction is performed using the chip area and the feature parameters of images with chip interference.

### 5.2 Validation process of the error corrected model

The 10 groups of images in the dataset are randomly selected to verify the error correction model. The verification results are shown in Table 2. Compared with

lot of training data and high-performance computing units. This increases algorithm training time and hardware costs, which is very disadvantageous for industrial applications [20]. On the other hand, the deep convolution neural network is suitable for feature extraction of the whole image. When the image surface is covered by interference factors, the extracted features will be invalid. Therefore, considering the practical application of industrial manufacturing process, this paper takes the BP neural network model and SVM model as the main research object. Then, the two prediction models are used to predict surface roughness using the optimized multi-dimensional feature parameter matrix as input. At the same time, the results of the two prediction models are compared and analyzed. Because the BP neural network and SVM model are widely used, their basic concepts will not be repeated.

### 6.1 Establishment of two prediction models

#### 6.1.1 Establishment of BP neural network prediction model

The input layer of the BP neural network is the four feature parameters in the multi-dimensional feature parameters matrix, namely, difference, contrast, entropy, and



**Table 2** Analysis of results after optimization of feature parameters

Number	Chip area (pixels)	Type	Differences	Contrast	Entropy	Energy ( $10^{-3}$ )
1	122,487	Original image	2.3725	14.2208	5.7397	5.6221
		Before optimization	2.1884	13.3460	5.5699	12.4654
		After optimization	2.5263	14.9609	5.7793	6.2605
2	162,845	Original image	2.3162	13.5032	5.5984	7.0946
		Before optimization	2.0674	12.3750	5.4114	19.8898
		After optimization	2.3576	14.2000	5.7018	8.2659
3	398,087	Original image	2.4363	14.6549	5.4956	8.0806
		Before optimization	1.7080	10.4351	4.4820	96.5523
		After optimization	2.3979	14.4507	5.4100	8.7504
4	260,822	Original image	2.3290	14.5346	5.5002	9.5909
		Before optimization	1.8319	11.1605	4.8742	42.3949
		After optimization	2.2554	13.6878	5.3795	9.0045
5	410,506	Original image	2.4749	15.9826	5.4038	9.2713
		Before optimization	1.6557	10.5386	4.3571	102.7221
		After optimization	2.3561	14.7839	5.3106	8.7164
6	461,828	Original image	2.3748	14.7976	5.5917	7.9856
		Before optimization	1.5346	9.5669	4.1915	139.3269
		After optimization	2.3174	14.2149	5.3359	9.1651
7	228,417	Original image	2.3776	13.6179	5.6925	7.5654
		Before optimization	1.8569	10.6458	5.0899	27.7084
		After optimization	2.2259	12.7512	5.5240	7.4031
8	363,225	Original image	2.3662	14.4276	5.5263	8.0261
		Before optimization	1.6937	10.4073	4.6123	81.5039
		After optimization	2.2928	13.9243	5.4256	8.9716
9	575,573	Original image	2.3628	15.4192	5.2490	8.7296
		Before optimization	1.2977	8.4354	3.7959	200.5781
		After optimization	2.2886	14.6385	5.4376	8.1608
10	653,982	Original image	2.5769	18.5996	5.6055	7.8377
		Before optimization	1.1842	8.6142	3.3826	267.7158
		After optimization	2.3823	17.1353	5.3717	8.2404

energy. The output layer is the surface roughness. The BP neural network selects a single hidden layer. According to empirical Equation (6) and experimental method, the optimal number of hidden layer nodes in the BP neural network model is 5. At the same time, the particle swarm optimization (PSO) algorithm is used to optimize the two main parameters  $w$  and  $m$  of the BP neural network ( $w$  and  $m$  refer to the initial weight and threshold of the optimal neural network respectively) [21, 22]. The optimization process follows two principles: one is high precision, but not over learning. The other is that regression data have a monotonic relationship with roughness.

$$s = \sqrt{m+n+a}, a \in [1, 10] \quad (6)$$

where  $m$  is the number of input layer nodes,  $n$  is the number of output layer nodes, and  $a$  is the coefficient.

The hidden layer transfer function of BP neural network is the tansig and the purelin of the output layer transfer function. The training function of BP neural network is trainlm. The training times is set at 5000, the learning rate is set at 0.0005, and the minimum error of the training target is set at 0.00001.

### 6.1.2 Establishment of the SVM model

The SVM proposed by Vapnik takes the training error as the constraint condition of the optimization problem and the minimization of the confidence range as the optimization objective [23, 24]. At the same time, the PSO algorithm is used to optimize the two main parameters  $c$  and  $g$  of SVM ( $c$  and  $g$  refer to penalty factor and Gaussian kernel function respectively). The optimization principle is consistent with the BP neural network process.

### 6.2 Surface roughness prediction based on two prediction models

This paper conducts error correction for feature parameters that change due to interference factors. Therefore, both models were trained using the non-interference surface image. The multi-dimensional feature parameter matrix of the non-interference surface image and its roughness values are used as input and output for model training. When encountering surface images with chip interference, the extracted multi-dimensional feature parameter matrices are optimized using the error correction model. The optimized multidimensional feature parameter matrices are separately input to the two trained prediction models for roughness prediction. The training of the two models is based on 200 non-interference sample surface images in the dataset. The validation of the two models is to use 25 surface images with chip interference in the dataset.

The detection results of BP neural network model and SVM model are shown in Fig. 7. The relative error of the prediction results of BP neural network model and SVM model does not exceed 15%, the average relative error is 7.91% and 8.64% respectively, and the average single detection time is 0.52 s and 0.73 s, respectively. The relative

prediction error and time of the BP neural network model are better than that of the SVM model by analyzing the prediction results. These results not only show that the multi-dimensional feature parameters matrix has a good prediction ability for surface roughness but also prove the effectiveness of the proposed error correction model and sustainable detection research from two aspects. The surface roughness sustainability detection process is shown in Fig. 8.

## 7 System integration of surface roughness sustainability measurement

### 7.1 Sustainability detection system

Sections 5 and 6 introduce the research process for the research on the sustainability detection of machined surface roughness under the influence of the industrial cutting environment. This section uses LabVIEW and MATLAB software to implement the system integration of this research process. The sustainability detection system includes both hardware and software. The hardware part is the built-in image acquisition device. The reason for constructing the image acquisition device is that the laser microscope cannot be applied directly to collect surface

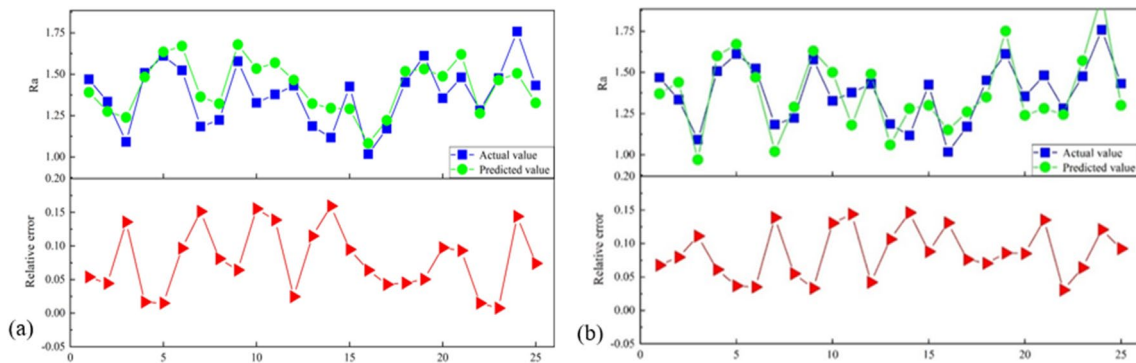
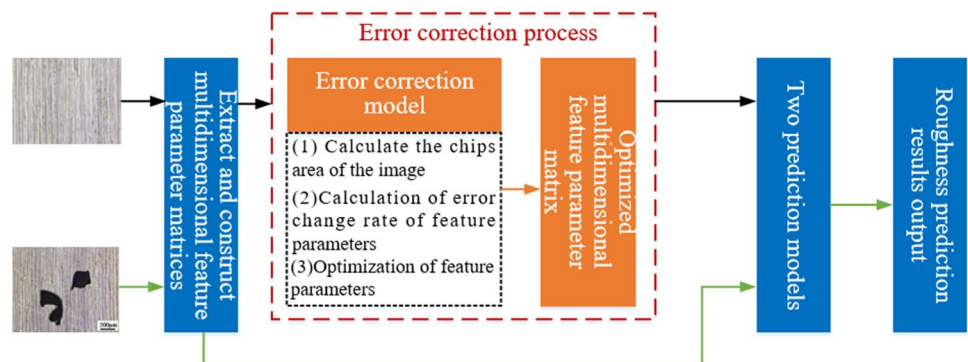
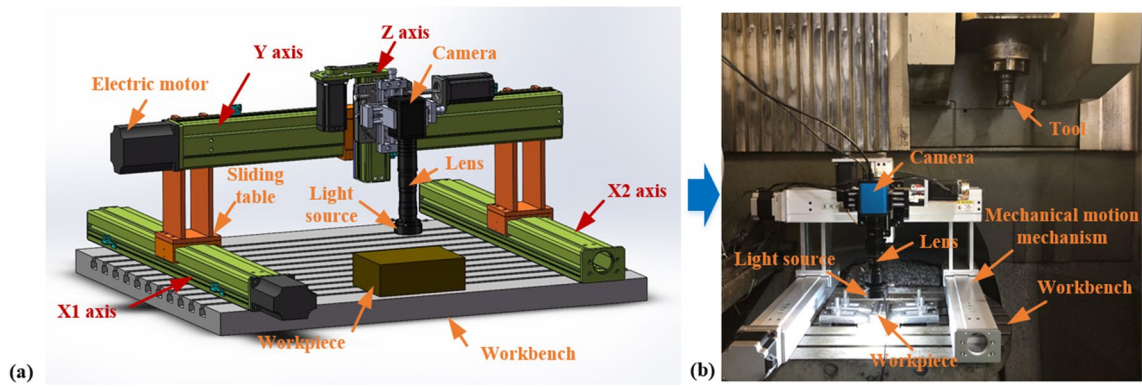


Fig. 7 Prediction results of the two prediction model. a The roughness prediction results of the images with chip interference based on the BP neural network model. b The roughness prediction results of the images with chip interference based on the SVM model

Fig. 8 The sustainability detection process of surface roughness



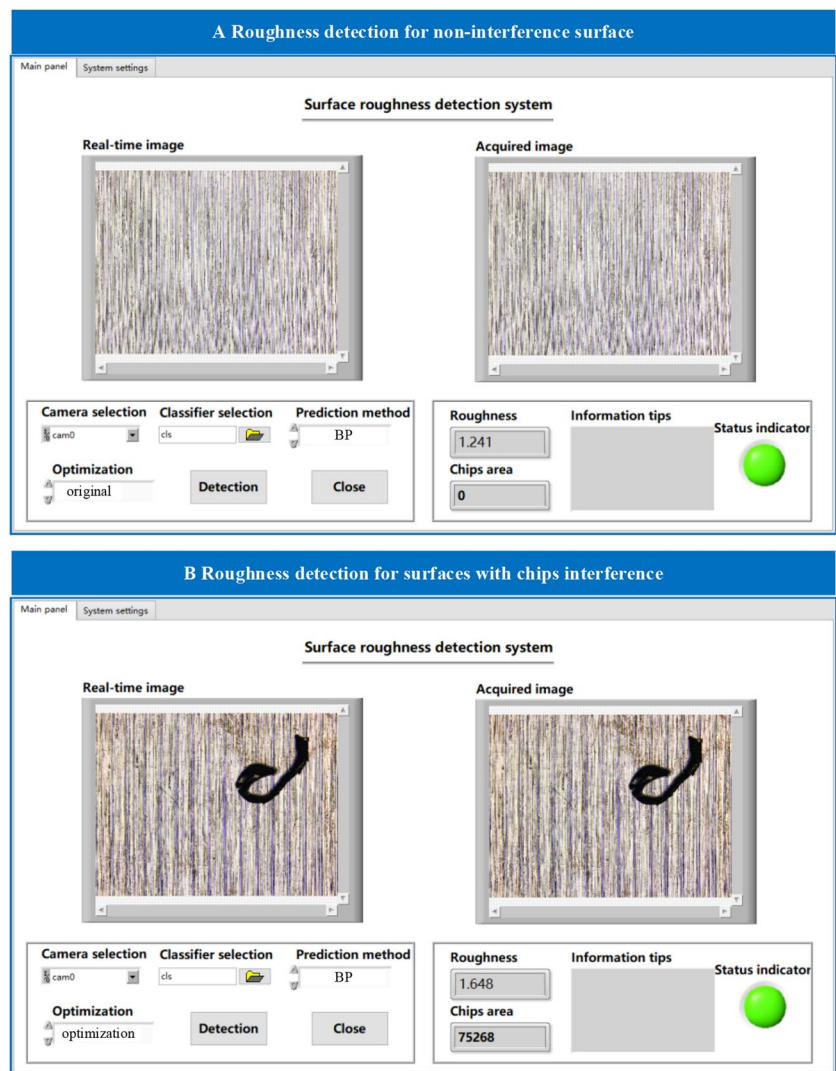


**Fig. 9** Image acquisition device. **a** Three-dimensional model of image acquisition device. **b** Work site of the image acquisition device

images in the actual cutting environment. The software part is the sustainability measurement method proposed in this paper. The hardware part can drive the camera to collect the image on the surface to be detected. The acquired images were transferred

to the software section. The roughness detection of the image is performed by the software part. Among them, the quality and texture structure of surface images collected by laser microscopes and image acquisition devices are basically the same.

**Fig. 10** The main interface of the software system

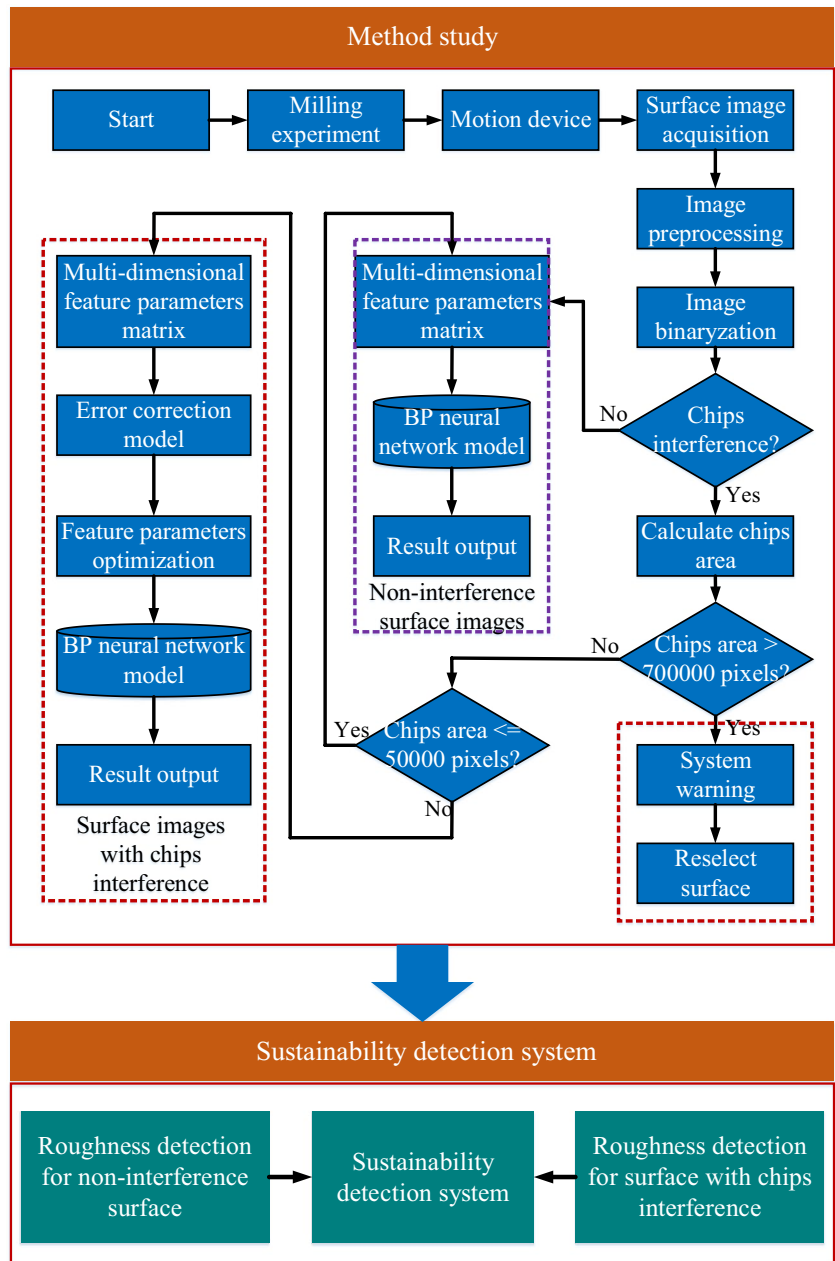


### 7.1.1 Image acquisition device

In order to obtain the surface image effectively in the actual industrial cutting environment, this section has built an image acquisition device. The three-dimensional model of the image acquisition device is shown in Fig. 9a. The image acquisition device is on the working site of the industrial manufacturing process, as shown in Fig. 9b. The image acquisition device is placed on the workbench of the machine tool without affecting the operation of the cutting tool. This ensures that the device can timely obtain the machined surface image after completion of the processing. The image acquisition device consists of a mechanical

motion mechanism, a camera, a lens, a light source, and a light source controller. The main advantage of this camera is the automatic focusing system. The camera can automatically focus and shoot even if the height of the target object changes. This ensures that the acquired surface will not be blurred due to the change in focal length. Its magnification is 30 to 200 times. The image acquisition function of the cameras is controlled by the computer. The camera is mounted on a mechanical motion mechanism. When the machine tool is working, the mechanical motion mechanism drives the image acquisition device away from the cutting area. When the spindle of the machine tool completes the work and leaves the cutting area, the mechanical motion mechanism

Fig. 11 Sustainability detection system



drives the image acquisition device to the surface of the workpiece for image acquisition.

### 7.1.2 The software part

The software part is to form the proposed research method into a system. It is not necessary to optimize the feature parameters to predict surface roughness for non-interference surface images, but it is necessary for surface images with chip interference. The interface of the software system is shown in Fig. 10.

## 7.2 Validation of the sustainability detection system

This part is aimed at verifying the performance of sustainability detection systems in industrial cutting environments. The sustainability detection system is controlled by the computer to collect the surface image after the cutting of the machine tool is completed. In this process, 20 surface images are collected and detected (10 non-interference surfaces and 10 surfaces with chip interference). The operation process of the sustainability detection system is shown in Fig. 11.

The detection results of the sustainability detection system are shown in Fig. 12a, b. The average relative error of the detection results for non-interference surface images and surface images with chip interference is 7.00% and 8.06%, and the average single detection time is 0.75s and 0.96s. This time is the process from camera shooting to the emergence of roughness results. This result satisfies the error and time requirements of fast roughness prediction. It has been shown that the sustainability detection system has good practical performance in cutting environment. This sustainability detection system provides technical support for the efficient automatic operation of industrial manufacturing processes.

## 8 Conclusion

Industrial manufacturing parts are moving towards complexity, small batching, and customization, and their economy and safety are increasingly valued. However, the detection of the surface quality of the machined surface is increasingly faced with the influence of interference factors (chips or coolant residue) in the complex environment. The existing detection methods have a large error due to interference factors. Therefore, in order to test the normal surface roughness under the influence of interference factors, this paper has carried out a study on the sustainability detection of surface roughness.

Sustainability detection research: based on the gray level co-occurrence matrix, a multi-dimensional feature parameter matrix with strong correlation with surface roughness is extracted and constructed. Then, the adverse changes of image feature parameters caused by interference factors (chips) are quantitatively analyzed. Further, the error correction model is constructed by using the relationship between chip area and error change rate of feature parameters, which realizes the optimization of the changed characteristic parameters. Finally, the BP neural network model and the SVM model are respectively used to predict surface roughness with the optimized multi-dimensional feature parameters matrix as the input, which verifies the effectiveness of the proposed error correction model and sustainability detection method.

Integration of sustainability detection system: LabVIEW software and MATLAB software are used for software system integration of sustainability detection research. The sustainability detection system is verified by using non-interference surface images and surface images with chip interference in the environment of the actual cutting process. The average relative error of validation results for non-interference surface images and surface images with

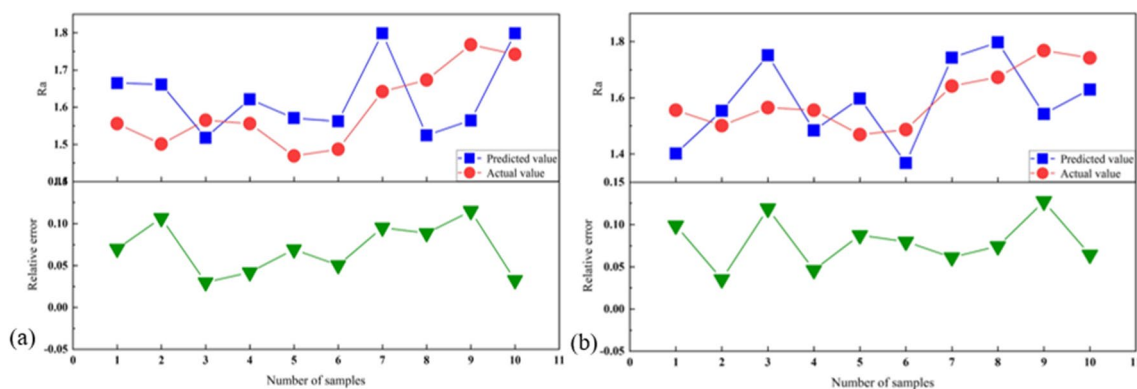


**Fig. 12** Detection results of sustainable detection system. **a** Roughness detection results for non-interference surface images. **b** Roughness detection results for surface images with chip interference

chip interference is 7.00% and 8.06%, and the average single detection time is 0.75s and 0.96s. These results prove the effectiveness and practicability of the sustainability detection system. This sustainability detection system realizes the rapid, anti-interference, and accurate detection of surface roughness in the industrial cutting process.

**Author contributions** Wei Chen (first author): methodology, validation, formal analysis, investigation, and writing original draft. Bin Zou (corresponding author): formal analysis, resources, and writing—review and editing. Qinbing Zheng and Chuanzhen Huang: formal analysis. Lei Li and Jikai Liu: check and verify original draft. The authors' contribution corresponds their order. All authors read and approved the final manuscript.

**Funding** This project was supported by the National Key Research and Development Project of China (2022YFB4601403) and the National Natural Science Foundation of China (No. 52175336).

**Data availability** The data that support the findings of this study are available from the corresponding author upon reasonable request.

## Declarations

**Ethics approval** This study does not involve human participants and/or animal studies.

**Consent for publication** Not applicable. All data in this paper can be published and verified by all authors. All the authors listed have approved the manuscript that is enclosed.

**Competing interests** The authors declare that they have no known competing financial interests or personal relationships that could have appeared to influence the work reported in this paper.

**Disclaimer** I would like to declare on behalf of my co-authors that the work described was original research that has not been published previously and not under consideration for publication elsewhere, in whole or in part.

## References

- Tian HY, Zhang LN, Dong JJ, Wu L, Fang FL, Wang YF, Li H, Xie CS, Li WJ, Wei ZB, Liu ZG, Zhang M (2022) A one-step surface modification technique improved the nutrient release characteristics of controlled-release fertilizers and reduced the use of coating materials. *J Clean Prod* 369:133331. <https://doi.org/10.1016/j.jclepro.2022.133331>
- Zhang H, Liu J, Chen SF, Wang WF (2018) Novel roughness measurement for grinding surfaces using simulated data by transfer kernel learning. *Appl Soft Comput* 73:508–519. <https://doi.org/10.1016/j.asoc.2018.08.042>
- Wang JP, Xu GL, Li CL, Wang ZS, Yan FJ (2021) Surface defects detection using non-convex total variation regularized RPCA with kernelization. *IEEE Trans Instr Measure* 70:5007013. <https://doi.org/10.1109/TIM.2021.3056738>
- Svalina I, Simunovic G, Saric T, Lujic R (2017) Evolutionary neuro-fuzzy system for surface roughness evaluation. *Appl Soft Comput* 52:593–604. <https://doi.org/10.1016/j.asoc.2016.10.010>
- Gupta MK, Song QH, Liu ZQ, Sarikaya M, Jamil M, Mia M, Singla AK, Khan AM, Khanna N, Pimenov DY (2021) Environment and economic burden of sustainable cooling/lubrication methods in machining of Inconel-800. *J Clean Prod* 287:125074. <https://doi.org/10.1016/j.jclepro.2020.125074>
- Zhao YJ, Yan YH, Song KC (2017) Vision-based automatic detection of steel surface defects in the cold rolling process: considering the influence of industrial liquids and surface textures. *Int J Adv Manuf Technol* 90:1665–1678. <https://doi.org/10.1007/s00170-016-9489-0>
- Balasundaram MK, Ratnam MM (2014) In-process measurement of surface roughness using machine vision with sub-pixel edge detection in finish turning. *Int J Precis Eng Manuf* 15(11):2239–2249. <https://doi.org/10.1007/s12541-014-0587-3>
- Tootooni MS, Liu C, Roberson D, Donovan R, Rao PK, Kong Z, Bukkapatnamd STS (2016) Online non-contact surface finish measurement in machining using graph theory based image analysis. *J Manuf Syst* 41:266–276. <https://doi.org/10.1016/j.jmsy.2016.09.007>
- Liu QY, Yu DJ, Wang CT, Li X (2015) Development of the online measuring system of grinding surface roughness based on DSP. *J Hunan Univ (Nat Sci)* 42(8):1–7. <https://doi.org/10.16339/j.cnki.hdxzbzkb.2015.08.001>
- Yi ZK, Zhang YL (2017) Recognizing tactile surface roughness with a biomimetic fingertip: a soft neuromorphic approach. *Neurocomputing* 244:102–111. <https://doi.org/10.1016/j.neucom.2017.03.025>
- He Y, Song KC, Meng QG, Yan YH (2020) An end-to-end steel surface defect detection approach via fusing multiple hierarchical features. *IEEE Trans Instr Measure* 69(4):1493–1504. <https://doi.org/10.1109/TIM.2019.2915404>
- Kumar A, Shankar R, Choudhary A, Thakur LS (2016) A big data MapReduce framework for fault diagnosis in cloud-based manufacturing. *Int J Prod Res* 54(23):7060–7073. <https://doi.org/10.1080/00207543.2016.1153166>
- Deng JH, Lu Y, Lee VCS (2020) Imaging-based crack detection on concrete surfaces using You Only Look Once network. *Struct Health Monitor* 20(2):484–499. <https://doi.org/10.1177/1475921720938486>
- Pashmforoush F, Bagherinia RD (2018) Influence of water-based copper nanofluid on wheel loading and surface roughness during grinding of Inconel 738 superalloy. *J Clean Prod* 178:363–372. <https://doi.org/10.1016/j.jclepro.2018.01.003>
- Liu Q, Huang W, Li LL, Zhao ZL (2020) Vibration-resistant interferometric measurement of optical surface figure and roughness. 6th Asia Pacific Conference on Optics Manufacture (1138304). <https://doi.org/10.1117/12.2523358>
- Yang JZ, Zou B, Guo GQ, Chen W, Wang XF, Zhang KH (2022) A study on the roughness detection for machined surface covered with chips based on deep learning. *J Manuf Proc* 84:77–87. <https://doi.org/10.1016/j.jmapro.2022.09.061>
- Yi HA, Liu J, Ao P, Lu EH, Zhang H (2016) Visual method for measuring the roughness of a grinding piece based on color indices. *Optics Express* 24(15):17215–17233. <https://doi.org/10.1364/OE.24.017215>
- Yi HA, Liu J, Lu EH, Peng AO (2016) Measuring grinding surface roughness based on the sharpness evaluation of color images. *Measure Sci Technol* 27(2):1–14. <https://doi.org/10.1088/0957-0233/27/2/025404>
- Haralick RM, Shanmugam K, Dinstein I (1973) Textural features for image classification. *Stud Med Commun SMC-3*(6):610–621. <https://doi.org/10.1109/tsmc.1973.4309314>
- Su H, Zhang JB, Zhang BH, Zou W (2021) Review of research on the inspection of surface defect based on visual perception. *Comp Integr Manuf Syst*:1–31 <https://kns.cnki.net/kcms/detail/11.5946.TP.20210428.1807.024.html>

21. Zhou JH, Ren JX, Yao CF (2017) Multi-objective optimization of multi-axis ball-end milling Inconel 718 via grey relational analysis coupled with RBF neural network and PSO algorithm. *Measurement* 102:271–285. <https://doi.org/10.1016/j.measurement.2017.01.057>
22. Ghosh G, Mandal P, Mondal SC (2019) Modeling and optimization of surface roughness in keyway milling using ANN, genetic algorithm, and particle swarm optimization. *Int J Adv Manuf Technol* 100(5-8):1223–1242. <https://doi.org/10.1007/s00170-017-1417-4>
23. Liu W, Tu XM, Jia ZY, Wang WQ, Ma X, Bi XD (2013) An improved surface roughness measurement method for micro-heterogeneous texture in deep hole based on gray-level co-occurrence matrix and support vector machine. *Int J Adv Manuf Technol* 69:583–593. <https://doi.org/10.1007/s00170-013-5048-0>
24. Grinblat GL, Uzal LC, Verdes PF, Granitto PM (2015) Nonstationary regression with support vector machines. *Neural Comput Appl* 26:641–649. <https://doi.org/10.1007/s00521-014-1742-6>

**Publisher's note** Springer Nature remains neutral with regard to jurisdictional claims in published maps and institutional affiliations.

Springer Nature or its licensor (e.g. a society or other partner) holds exclusive rights to this article under a publishing agreement with the author(s) or other rightsholder(s); author self-archiving of the accepted manuscript version of this article is solely governed by the terms of such publishing agreement and applicable law.